Support Information

Synergistic Effects of Precursor Reduction and Ion Migration Blocking Enable Highly Sensitive $MAPbI_3$ X-ray Detector with Low Detection Limit

Long Jiang,[1*#] *Chengzhi Xue*,[2#] *Jiantian Cheng*,[2] *Nan Li*,[2] *Xinyu Fan*,[2] *Yuanbo Yang*,[1] *Tiantian Li*,[1] *Liwei Li*,[1] *Yucheng Liu*,[2] *Jiangshan Feng*,[2] *Shengzhong (Frank) Liu*,[3, 4*] *and Zhou Yang*[2*]

1. State Key Laboratory of Oil and Gas Equipment, CNPC Tubular Goods Research Institute, Xi'an, Shaanxi 710077, China.

2. Key Laboratory of Applied Surface and Colloid Chemistry, Ministry of Education, Shaanxi Key Laboratory for Advanced Energy Devices, Shaanxi Engineering Lab for Advanced Energy Technology, School of Materials Science and Engineering, Shaanxi Normal University, Xi'an 710119, China

3. University of Chinese Academy of Sciences, Dalian Institute of Chemical Physics, Chinese Academy of Sciences, Dalian, 116023, China

4. Dalian National Laboratory for Clean Energy, iChEM, Dalian Institute of Chemical Physics, Chinese Academy of Sciences, Dalian, 116023, China

# These two authors contribute equally.

Corresponding authors:

Long Jiang jianglong003@cnpc.com.cn

Shengzhong (Frank) Liu szliu@dicp.ac.cn

Zhou Yang zyang@snnu.edu.cn

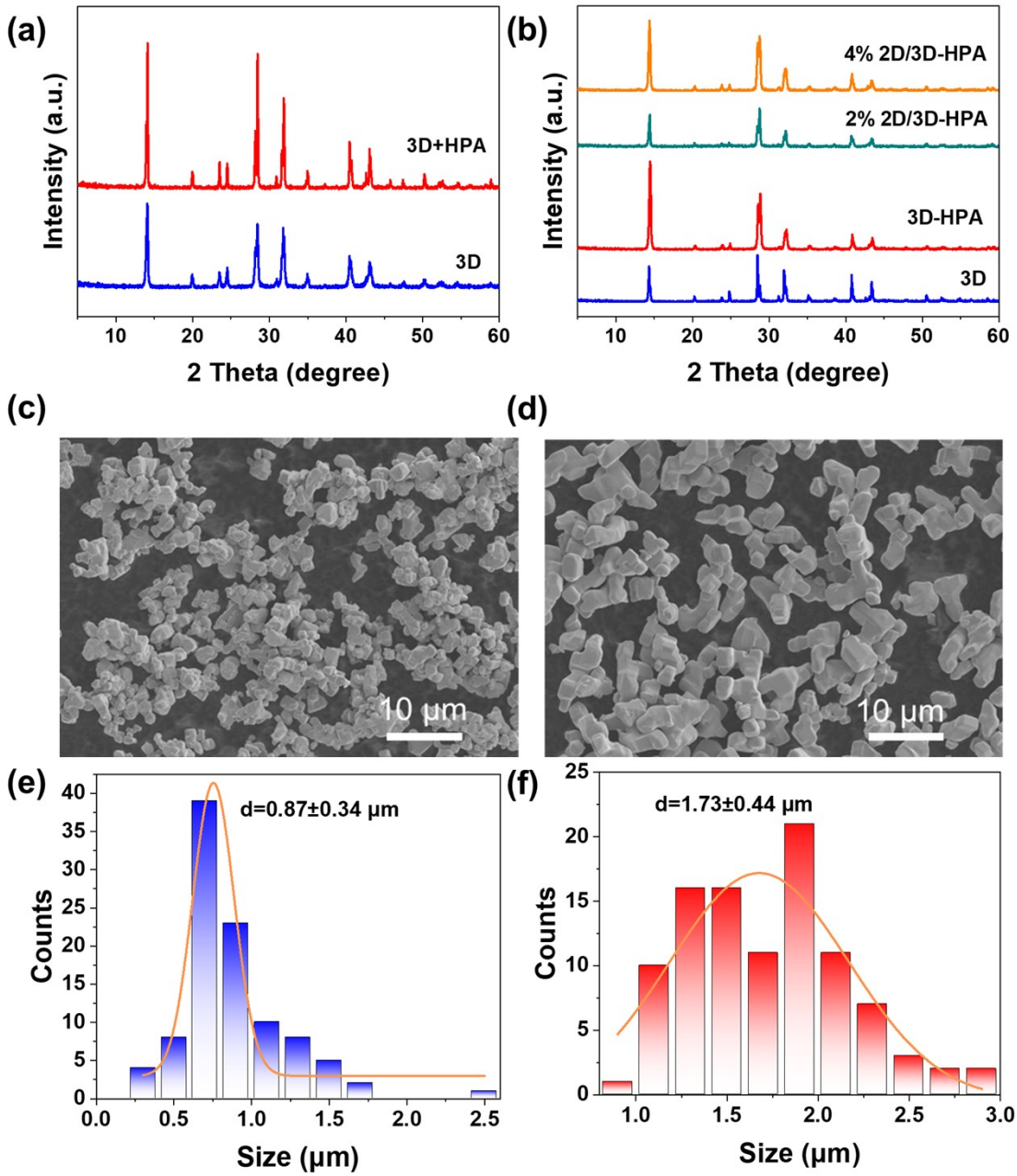

Figure S1. XRD patterns of (a) 3D and 3D-HPA samples; (b) XRD patterns of 3D, 3D-HPA and samples with *g*-C_3N_4; the morphologies of obtained powders with (c) and without the addition of HPA (d); Grain size statistics of 3D and 3D-HPA samples.

Figure S2. The photo picture during measuring the thickness of the pellet.

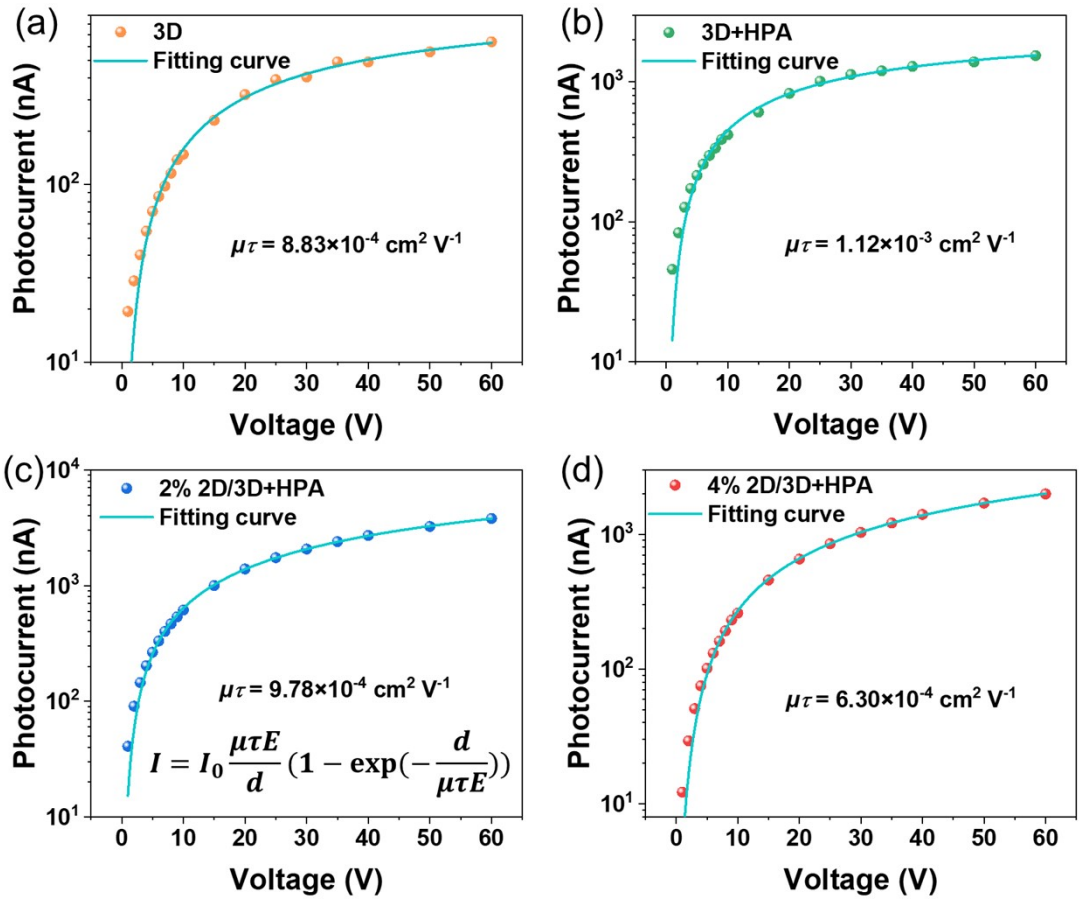

Figure S3. Photoconductivity of wafers and fitting lines for the $\mu\tau$ product (a) 3D wafer; (b) 3D-HPA wafer; (c) 2% 2D/3D-HPA wafer; (d) 4% 2D/3D-HPA wafer. The modified Hecht's equation (as inserted in panel c) was used to fit the obtained data.

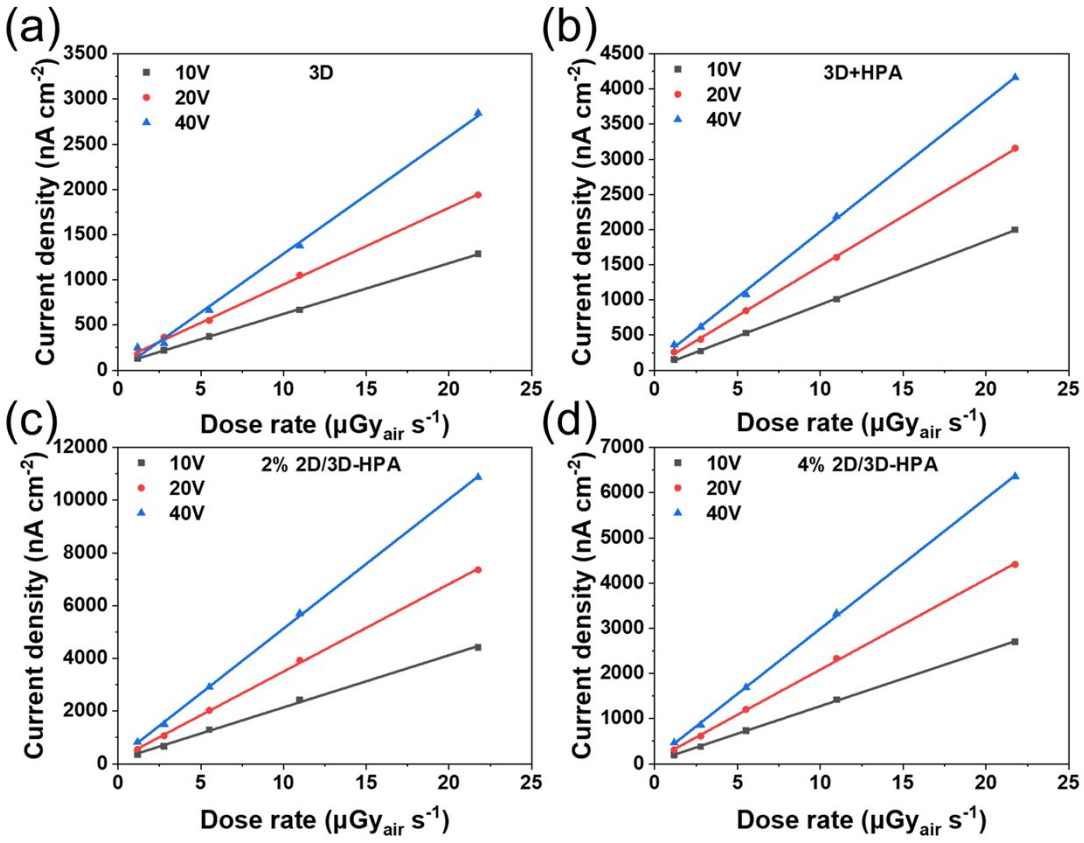

Figure S4. The dose rate depended photocurrent responses of $MAPbI_3$ pellets: (a) 3D pellet, (b) 3D-HPA pellet, (c) 2% 2D/3D-HPA pellet and (d) 2% 2D/3D-HPA pellet. These data were used to estimate the X-ray sensitivities of $MAPbI_3$ pellets.

Table S1. Summary of the performance of perovskite-based X-ray detectors.

Material	Sensitivity ($\mu C\ Gy_{air}^{-1}\ cm^{-2}$)	Detection limit ($nGy_{air}\ s^{-1}$)	X-ray source	Ref
$((NH_2)_2CNHNH_2)_3Bi_2I_9$ wafer	2675@66 V mm^{-1}	11.8	40 kV	[1]
$MAPbI_3$/Carbon Heterojunction thick film	142000 @1 V	48	40 kV	[2]
$CsPbBr_3$ thick film	42000@40 V mm^{-1}	136	60 kV	[3]
$MAPbI_3$ thick film	405937@5V	77	40 kV	[4]
$MAPbI_{3-x}Cl_x$ thick film	13000@12.5 V mm^{-1}	14.7	100 kV	[5]

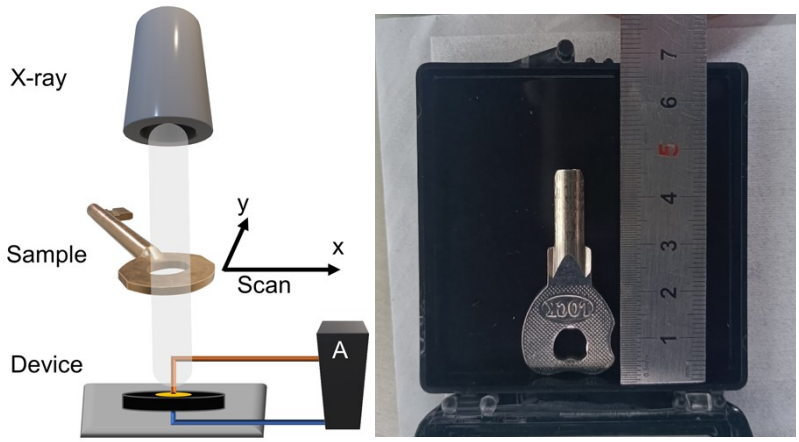

Figure S5 (a) Device for X-ray imaging tests; (b) Photographs of the key used for imaging.

Reference

[1] J. Yu, Y. Luo, N. Tian, Y. Liu, Z. Yang, J. Pi, L. Li, R. Zheng, C. Wang, S. (Frank) Liu, *Adv. Mater.* DOI: 10.1002/adma.202413709.

[2] Y. Zhang, Z. Huang, C. Peng, N. Gao, X. G. Xu, Y. Li, C. Zheng, W. Chen, Y. Yang, J. Zhao, J. Yang, T. Chen, Z. Xiao, *Nat. Commun.* **2024**, *15*, 10311.

[3] J. Wang, S. Yu, H. Jin, Y. Li, K. Zhang, D. L. Phillips, S. Yang, *Adv. Sci.* **2024**, *11*, 2407314.

[4] X. Qin, J. Han, Y. Chai, B. Cao, A. Li, H. Zeng, X. Li, *ACS Appl. Mater. Interfaces* **2024**, *16*, 55705.

[5] Z. Zhu, H. Chen, W. Huang, B. Zhao, S. Gao, Y. He, G. Zhong, X. Yang, X. Wang, Y. Li, *ACS Appl. Mater. Interfaces* **2024**, *16*, 53177.